Curing of Epoxy–Urethane Copolymers in a Heated Mold: Effect of the Curing Conditions on the Phase-Separation Process

P. M. STEFANI,[1] S. M. MOSCHIAR,[1] M. I. ARANGUREN,[1] C. MARIETA,[2] I. MONDRAGON[2]

[1] Institute of Material Science and Technology (INTEMA), University of Mar del Plata–National Research Council (CONICET), Av. Juan B. Justo 4302, 7600 Mar del Plata, Argentina

[2] Departamento Ingeniería Química y Medio Ambiente, Escuela Universitaria Ingeniería Técnica Industrial, Universidad País Vasco/Euska Herriko Unibersitatea, Av. Felipe IV 1B, 20011 Donostia, Spain

Received 17 July 2000; accepted 22 October 2000

ABSTRACT: The curing process of an epoxy–urethane copolymer in a heated mold was studied. The epoxy resin (DGEBA, Araldyt GY9527; Ciba Geigy), was coreacted with a urethane prepolymer (PU, Desmocap 12; Bayer) through an amine that acted as crosslinking agent (mixture of cycloaliphatic amines; Distraltec). The study focused on the effect of the curing condition and PU concentration on time–temperature profiles measured in the mold and the consequent final morphologies obtained. As the PU concentration increases, the maximum temperature reached in the mold decreases as a result of the dilution effect of the elastomer on reaction heat, whereas the T_g of the piece also decreases. Phase separation is a function of conversion and temperature reached in the curing part and was analyzed using experimental data and a mathematical model that predicts temperature and conversion throughout the thickness of the mold. Scanning electron microscopy and atomic force microscopy were used to determine the characteristics of the dispersed phase for the different formulations and conditions of curing. It was shown that the size of the dispersed phase increased with the initial PU concentration, whereas there were practically no differences in the separated phase as a function of position or temperature of curing (in the range of 70 to 100°C studied). The superposition of the phase diagrams with the conversion–temperature trajectories during cure provided an explanation of the morphologies generated. © 2001 John Wiley & Sons, Inc. J Appl Polym Sci 81: 889–900, 2001

Key words: modified epoxy; epoxy–urethane copolymers; curing in mold; phase separation

INTRODUCTION

It is well known that amine-cured epoxy resins have low fracture resistance and to increase their toughness, they are combined with an elastomeric second phase.[1–12] The most common method used to introduce the second phase is to dissolve liquid elastomers in the amine/epoxy mixture, which become phase separated during the polymerization. The reactive mixture remains homogeneous until a certain extent of reaction is reached (cloud-point conversion). At this point a modifier-rich phase is segregated in the form of particles of a few micrometers in size.[13] Then, the phase separation

Correspondence to: M. Aranguren.

Contract grant sponsor: CONICET (National Research Council of Argentina).

Journal of Applied Polymer Science, Vol. 81, 889–900 (2001)

process can be arrested by gelation of the epoxy network.[13–16] The competence between the phase separation process and the chemical reaction determines both the morphology and the properties of the final thermoset. This balance is affected by solubility, initial concentration, and reactivity of the elastomer, as well as by the cure conditions. As previously reported in the literature, the greater the initial concentration of elastomer,[14] the lower the miscibility of the system.[17] Moreover, the lower the concentration of reactive groups in the modifier,[18] the greater the volume fraction of dispersed phase that is obtained.

During the cure of these modified systems in a heated mold, phase separation profiles may be developed, resulting from differences in the conversion–temperature–time histories, which are functions of the position in the mold. Fang et al.[19] studied the cure in a heated mold of castor oil–modified amine–epoxy mixture. This system exhibited upper critical solution temperature (UCST) behavior (the miscibility increases with temperature). They showed that under particular conditions of cure there was phase separation near the wall, whereas the core of the sample remained homogeneous (transparent). This particular morphology was analyzed using the temperature–conversion profile trajectories followed during the cure, together with a conversion–temperature phase diagram. Consequently, to obtain a thermoset piece with uniform morphology and properties, it is necessary to select the cure conditions to obtain similar conversion–temperature trajectories for the different positions in the piece.

The aim of this study is to explain and predict the final morphologies generated in an epoxy–urethane copolymer cured in a heated mold, with varying percentages of modifier and curing conditions. Experimental temperature–time profiles were measured during cure. A simple mathematical model that predicts temperature and conversion histories throughout the thickness of the mold was used to relate overall calorimetric conversion with experimental time. The simultaneous analysis of conversion–temperature trajectories with phase diagrams was used to explain the morphologies and thermal properties in the thermoset piece.

EXPERIMENTAL

Materials

The epoxy resin is a DGEBA (diglycidyl ether of bisphenol A; weight by epoxy equivalent: 189.8 g) ARALDIT GY 9527 from Ciba Geigy Co. (Summit, NJ). The hardener is a commercial mixture of cycloaliphatic diamines (weight per amine equivalent: 59.5 g; Distraltec, Argentina). The modifier is a commercial elastomer based in linear polyurethane Desmocap 12 (Bayer, Argentina); weight by isocyanate (NCO) equivalent: 2470 g], with terminal isocyanate groups blocked with an alkylphenol.

Testing Methods

Figure 1 shows a scheme of the air-heated glass mold used for the cure of all the samples studied. The reactive mixture was cast into the mold at room temperature. Then, the mold was placed inside a programmable oven (Memert ULP 500, Germany) at a selected constant temperature. Alumel–chromel thermocouples were used to monitor the temperature evolution, at different positions of the sample thickness.

The glass-transition temperatures (measured at the onset of the transition) of different epoxy–urethane copolymers were determined using a differential scanning calorimeter (Shimadzu DSC 50; Japan) at a heating rate of 10°C/min in nitrogen atmosphere.

Transmission optical microscopy (TOM) measurements were performed with an Olympus BHT-M microscope (Olympus, Lake Success, NY), equipped with a photoelectric cell. The time at which phase separation began (i.e., cloud-point time for a particular sample and curing temperature), t_{CP}, and the interval of time for phase separation to occur, Δt_{CP}, were determined from the light transmission recorder at different constant cure temperatures. The cloud-point time t_{CP} was determined at the onset of the light transmission decrease.

A set of thin tubes containing modified and pure epoxy–amine reactive samples was immersed in an oil bath kept at constant temperature. Gelation times t_{GEL} were measured by gently pulling a thin wire, immersed in the sample, taking t_{GEL} as the time at which the whole tube was lifted by pulling the wire.

The morphology of the epoxy–urethane copolymers was studied using scanning electron microscopy (SEM) and atomic force microscopy (AFM). The specimens for the analysis were fractured in air immediately after immersing them in liquid nitrogen. The micrographs were taken at the center and wall positions of the sample. The SEM photographs of the fracture surface were taken with a scanning electron microscope (model

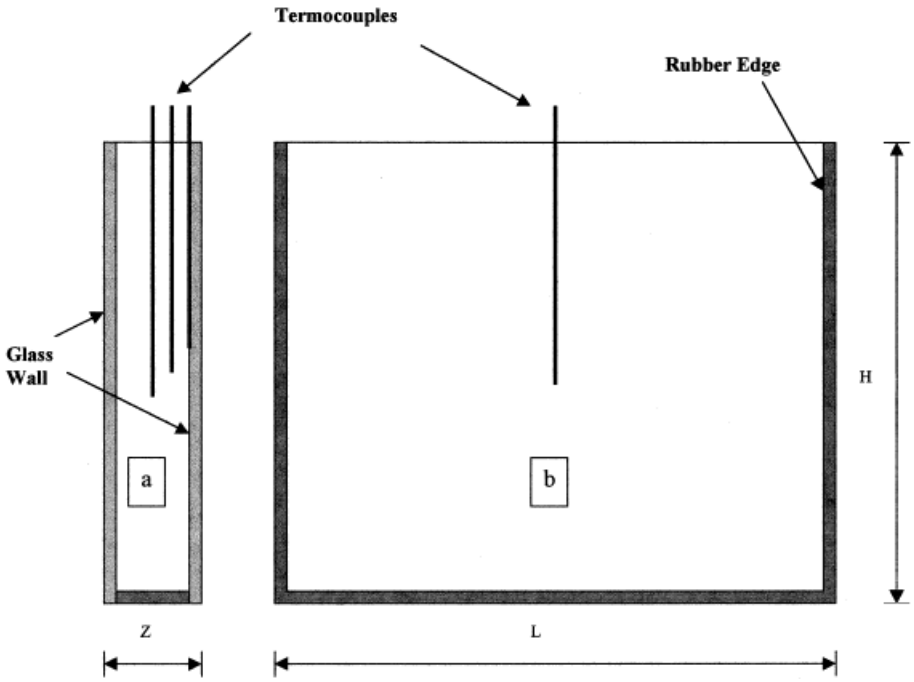

Figure 1 (a) Edge view of glass mold used in the curing process. (b) Front view of the mold. Dimensions: $Z = 1$ or 2 cm; $L = 15$ cm; $H = 12$ cm.

SEM 505; Philips, The Netherlands). The analysis by AFM was carried out using scanning probe microscopy (NanoScope IIIa, Multimode; Digital Instruments). The AFM was operated under ambient conditions using the contact mode. Table I provides information about the characteristics of the probe tips used. All images are shown without any image processing.

Mathematical Model

Phase separation as a function of conversion and temperature in the curing part was analyzed using experimental data and a simple mathematical model that predicts temperature and conversion throughout the thickness of the mold. This type of theoretical calculation has been the subject of several publications[19–23] and thus only a concise description of the procedure will be provided here.

Table I Characteristics of the Probe Tips Provided by Digital Instruments

Material	Silicon nitride
Cantilever configuration	V-frame
Cantilever length	200 μm
Cantilever thickness	0.4–0.6 μm
Cantilever width	35–40 μm
Spring constant	0.12 N/m
Nominal tip radius of curvature	20–40 nm

The following assumptions were adopted to solve this model:

- Homogeneous system: there is good mixing at initial time
- The diffusion of reactants in the mold is neglected
- One-dimensional heat conduction
- Constant thermal and physical properties (α, ρ, ΔH, C_p)

The mass (reaction rate) and energy equations in the curing polymer must be solved as a function of time:

$$\frac{\partial T}{\partial t} = \alpha \frac{\partial^2 T}{\partial z^2} + \frac{\Delta H_r}{C_p} R \quad \text{(energy balance)} \quad (1)$$

$$\frac{dx}{dt} = R \quad \text{(reaction rate)} \quad (2)$$

where

$$\alpha = \frac{k}{\rho C_p} \quad (3)$$

These equations relate conversion (x) and temperature (T) as functions of time (t) and position in the mold thickness (z), for given values of reaction heat (ΔH_r), thermal diffusivity (α), heat capacity (C_p), average density (ρ), and reaction rate (R).

Boundary Conditions

$$\frac{dT}{dz} = 0 \quad \text{at } z = \tfrac{1}{2}\,\text{thickness}$$

(symmetry at the center of the piece)

$$T = T_W \quad \text{at } z = 0 \quad \text{(at the wall)}$$

The values of T_W were obtained from the experimental temperature–time profiles at the wall of the mold.

Initial Conditions

$$T = T_O; \quad x = 0 \quad \text{at } t = 0 \quad \forall\, z$$

Kinetic Model

The study of the kinetics of the reaction epoxy–amine–PU has been the subject of a previous publication[24]; thus, only a brief summary is included in this work. The overall reaction rate is represented using a phenomenological model that includes the effect of the diffusion control at high conversions:

$$\frac{dx}{dt} = k_O x^m (1 - x)^n \tag{4}$$

The overall rate constant (k_O) was approximated with the Rabinowitch expression.[25] This equation considers that the overall time for the reaction is the sum of the time required for the diffusion of the reactants and that of the chemical reaction, as follows:

$$\frac{1}{k_O(x,\,T)} = \frac{1}{k_C(T)} + \frac{1}{k_D(x,\,T)} \tag{5}$$

where k_C and k_D are the rate constants of the chemically and diffusion-controlled reaction steps, respectively.

An Arrhenius type of equation was used to represent the functionality of k_C with the temperature:

$$k_C = A\,\exp\left(-\frac{E_C}{RT}\right) \tag{6}$$

where A is the preexponential constant, E_C is the kinetic activation energy, and R is the gas constant.

To represent the temperature dependence of the diffusion rate constant, the Adam–Gibbs[26] theory was used in the following equation:

$$\ln k_D = \ln k_{DO} - \frac{\ln 2E_D}{\Delta C_p T_c \ln \dfrac{T_c}{T_g - 50}} \tag{7}$$

where E_D is the diffusion activation energy, k_{DO} is the preexponential constant, and ΔC_p is the change in the specific molar heat of the sample at T_g.

Di Benedetto's[27] equation was used to relate T_g and the conversion of the partly cured reacting mixture:

$$\frac{T_g - T_{g0}}{T_{g\infty} - T_{g0}} = \frac{\lambda x}{1 - (1 - \lambda)x} \tag{8}$$

where T_{g0} and $T_{g\infty}$ are the glass-transition temperatures of the system at the initial time and complete conversion, respectively. λ was calculated as $T_{g0}/T_{g\infty}$ following the work of Pascault and Williams.[28,29] This is a rough approximation that was also used in the past in the absence of experimental values for the system.[30,31]

Differential equations were solved using an explicit method of finite differences. The parameters and physical properties used in the calculations are summarized in Table II.

RESULTS AND DISCUSSION

Curing in a Heated Mold

Samples of epoxy–amine and epoxy–amine–urethane copolymers were cured in heated molds of different thicknesses at fixed oven temperatures and at varying concentrations of PU in the copolymers. Composition, thickness, and curing conditions of specimens prepared are summarized in Table III.

Figures 2 to 4 show the temperature evolution at two thickness locations (wall and center), for the epoxy–amine (EA) and epoxy–urethane–amine (EA–PU) copolymers at different oven temperatures.

Three steps can be distinguished during the curing process:

Table II Physical Properties for the Pure and Modified Epoxy–Amine Systems

Property	System		
	Epoxy–Amine (EA)	EA + 10 wt % D12	EA + 20 wt % D12
ρ (kg/m^3)	1140	1135	1127
C_p (J/kg °C)[a]	2400	2300 (2200)[b]	2100 (2000)[b]
$\alpha \times 10^{-8}$ (m^2/s)[c] (for $T < T_{max}$)	6.7	7.2 (7.6)	7.6 (8.4)
$\alpha \times 10^{-8}$ (m^2/s)[c] (for $T > T_{max}$)	10	10	10
E_C (kJ/mol)	52.06	48.88	43.32
q	731.04	577.21	401.44
ln A (s^{-1})	11.18	10.23	8.16
ln k_{DO} (s^{-1})	11.44	13.04	10.37
ΔH_r (J/g)	371.2	353.9	307.8
$T_{g\infty}$ (K)	403	396	390.6
T_{g0} (K)	241	240	239
m	0.34	0.31	0.315
n	1.66	1.69	1.685

Kinetic parameters are from Stefani et al.[24]

[a] Measured by DSC. A constant C_p value was adopted, averaged in the temperature interval of curing process.

[b] C_p values in parentheses where used in the calculations for oven temperature of 30°C, since the range of temperature during curing is very different (lower) from that of the other higher temperature runs.

[c] α values are best-fitting parameters. Values are comparable to literature data for similar systems.[19]

1. Heating of the reactive mixture, when the temperature of the reactive mixture is lower than the temperature of the heating air. In this step, the wall temperature is higher than the temperature at the center of the part.
2. Heating of the polymer resulting from the generated heat of reaction. The rate of heat generated during the curing reaction is greater than the rate of heat conduction toward the mold walls and, then, a maximum in temperature occurs at the center of the piece.
3. A cooling period, which follows when the rate of heat generated inside the piece is lower than the conduction rate.

Table III Conditions of Curing and Thicknesses of the Samples

Desmocap 12 (wt %)	Oven Temperature (°C)	Thickness of Mold (cm)
0	50	1
	70	1
	70	2
	100	1
10	30	2
	70	1
	100	1
20	30	2
	70	1
	100	1

The maximum of temperature in the center of the mold is the result of two competing factors: (1) the rate of heat generated by the exothermic curing reaction and (2) the conductive heat flux toward the walls. The larger the ratio of the first factor, with respect to the second factor, the higher the maximum temperature reached by the sample in the mold. Many previous publications described the effect of the processing conditions on these two factors[20,21]; that is, the maximum temperature in the center of the piece will be higher if the external oven temperature, the heat of reaction, or the thickness of the mold are higher and it will be lower if the thermal conductivity is higher.

The effect of the oven temperature for these systems is shown in the temperature–time curves of Figures 2 to 4. The effect of the sample thickness is illustrated in Figure 5. The maximum temperature of the peak is approximately 80°C higher when the thickness is increased from 1 to 2 cm at the same external temperature.

At a fixed oven temperature of 70°C [Figs. 2(b), 3, and 4], the maximum temperature at the center of the mold decreases with the addition of the PU elastomer (the maximum temperatures

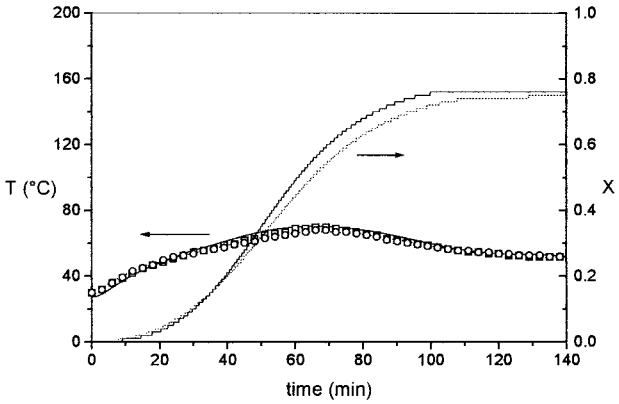

(a)

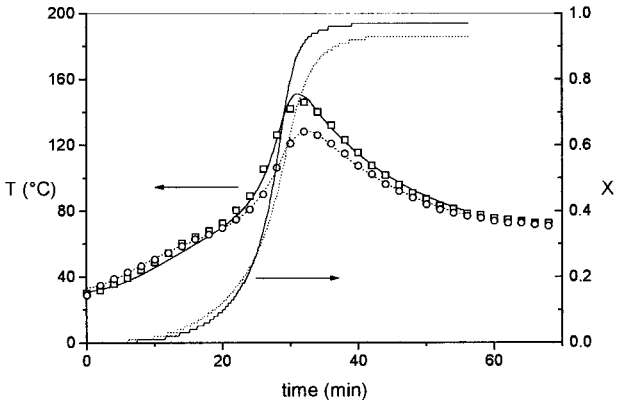

(b)

Figure 2 Epoxy–amine system. Thickness of the plaques: 1 cm. The symbols indicate experimental measurements. The lines are the results of the model. Temperature–time curves: (○, - - - -) wall; (□, —) center. Conversion–time curves: (- - - -) wall; (—) center. Oven temperatures: (a) 50°C; (b) 70°C.

reached in the center of the plaques are 151, 140, and 128°C for 0, 10, and 20 wt % of Desmocap 12, respectively). This can be explained as the dilution effect of the modifier on the copolymerization reaction heat, as previously reported.[24]

The glass-transition temperatures (T_g's) measured in the center and the wall of the different plaques are shown in Table IV. In all cases, the T_g measured in the center of the piece is higher than that at the wall, which is the result of the higher temperature reached in the center of the mold during the cure. A lower T_g is observed when the amount of modifier increases (for a given position in the mold and for a fixed oven temperature), in complete agreement with the lower temperatures reached during the cure and the elastomer effect on the thermoset transition (PU dilution effect as

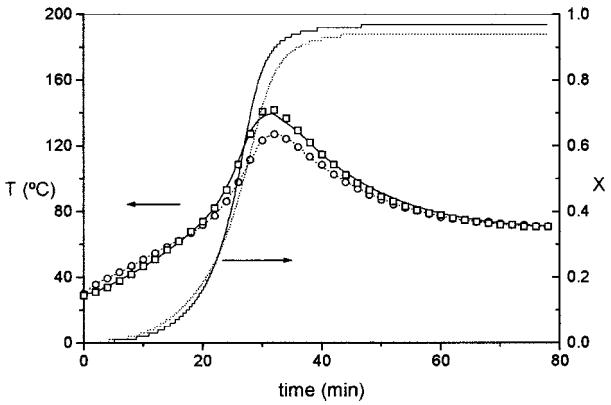

Figure 3 Epoxy–amine–10 wt % Desmocap 12 system. Symbols and lines have the same meaning as in Figure 2. Oven temperature: 70°C; thickness: 1 cm.

explained earlier). The values of $T_{g\infty}$ for the modified networks are also shown in Table IV. The lower $T_{g\infty}$'s, with respect to the neat epoxy–amine system, are the result of the copolymerization with PU.

Figures 2 to 4 also show the excellent fit between the results of the model and the experimental temperature–time profiles. The model also allows calculation of the overall calorimetric conversion–time profiles in the part. At short times, the conversion at the wall increases faster than at the center of the mold. As the curing reaction proceeds, the conversion at the center overcomes the conversion at the wall. The higher conversion reached at the center of the piece is the direct cause of the higher T_g measured in that position. Besides, this model can effectively predict the vitrification of all the systems studied when the

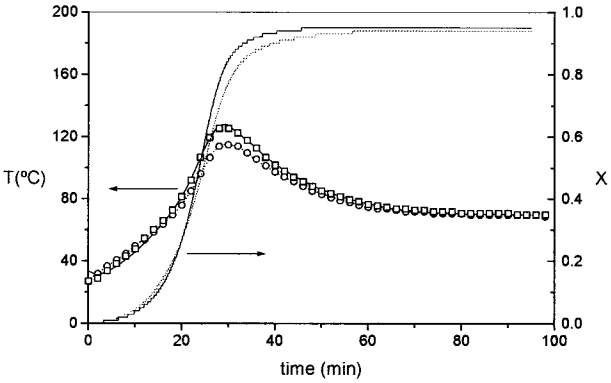

Figure 4 Epoxy–amine–20 wt % Desmocap 12 system. Symbols and lines have the same meaning as in Figure 2. Oven temperature: 70°C; thickness: 1 cm.

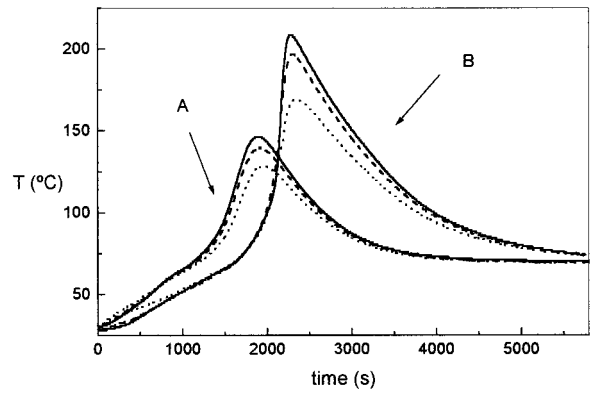

Figure 5 Temperature–time experimental curves for the epoxy–amine system. Oven temperature: 70°C. (· · ·) glass–polymer interface (wall); (- - - -) $\frac{1}{4}$ thickness; (—) $\frac{1}{2}$ thickness (center). (A) thickness: 1 cm, (B) thickness: 2 cm.

oven temperature is low, as shown by the low final conversion reached [Fig. 2(a)].

Cloud-Point Conversion

The gelation time, cloud-point time, and time interval for the phase separation process for epoxy–amine systems with 10 and 20 wt % of modifier at different curing temperatures are shown in Table V. To relate these times to conversions, the kinetic model already described[24] was used. Thus, the experimental data (time versus temperature) were converted to conversion versus temperature by means of this calculation. It is clear in Figure 6(a) and (b), that the cloud-point conversion decreases with the addition of elastomer for all the cure temperatures. The curve of x_{CP} versus curing temperature shows an intercept with the x_{gel} line. This intercept occurs at 50°C and around 45°C for the samples with 10 and 20 wt % of Desmocap 12, respectively. This indicates that the sample with the lower concentration of Desmocap 12 can produce a transparent material up to slightly higher temperatures than that of the 20 wt % Desmocap 12 sample. In both cases, the cloud-point conversion decreases with increasing cure temperature until an approximately constant value is reached at a temperature of about 80°C.

The higher the cure temperature, the faster the reaction rate and, then, higher conversions are achieved at shorter times. The kinetic rate shows a stronger dependency on the temperature than on the diffusion process. Large molecules do not diffuse fast enough to maintain the system homogeneity during the reaction, and phase separation occurs at a lower conversion. At higher temperatures this effect is less important (x_{CP} is approximately constant at cure temperatures $\geq$ 85°C), probably as a result of the relatively small size of the structures present at low conversion, which consequently can diffuse faster. At temperatures higher than 80°C, at the end of the phase separation process, the conversion of the sample with 20 wt % of Desmocap 12 is smaller than the gelation conversion. This means that, in these conditions, the gelation does not arrest the phase-separation process. However, at lower temperatures it is observed that the phase separation process is arrested because of diffusional restrictions[32] by vitrification or gelation (at $T < {}_{\text{gel}}T_g$ or $T > {}_{\text{gel}}T_g$, respectively). This last feature is observed at all the cure temperatures utilized for the samples with 10 wt % of Desmocap 12.

Morphology of the Plaques

Fracture surfaces of copolymers with 10 and 20 wt % of modifier and cured at different oven temperatures (T_o) were studied. Samples cured at 70 and 100°C were completely opaque, indicating that the phase separation process took place at every position, although those cured at T_o = 30°C were completely transparent. Figure 7 shows the

Table IV T_g of Plaques for the Pure and Modified Epoxy–Amine Systems

Sample	T_o[a] (°C)	Position	Thickness (cm)	T_g (°C)
Epoxy	50	Center	1	60
($T_{g\infty}$ = 130°C)	50	Wall	1	60
	70	Center	1	91
	70	Wall	1	87
	100	Center	1	122
	100	Wall	1	110
Epoxy–10 wt % D12	30	Center	2	53
($T_{g\infty}$ = 124°C)	30	Wall	2	52
	70	Center	1	97
	70	Wall	1	86
	100	Center	1	109
	100	Wall	1	103
Epoxy–20 wt % D12	30	Center	2	53
($T_{g\infty}$ = 118°C)	30	Wall	2	54
	70	Center	1	85
	70	Wall	1	80
	100	Center	1	98
	100	Wall	1	99

[a] T_o, oven temperature.

Table V Cloud-Point, Phase-Separation Interval, and Gelation Times in Minutes for the Pure and Modified Epoxy–Amine Systems

Cure Temperature (°C)	EA t_{GEL}	EA + 10 wt % D 12			EA + 20 wt % D12		
		t_{GEL}	t_{CP}	Δt_{CP}	t_{GEL}	t_{CP}	Δt_{CP}
50			91	14		61	17
60			46	9		32	12.4
70	33	31	25.5	7.6	31	21	8.4
85	19	18	11.2	6.2	16	9.1	3.4
100	10	10	6.4	3.4	9.5	5	1.8

fracture surface of this sample that indicates the presence of a single phase and the features typical of brittle fracture in a homogeneous material. Figure 8 shows the SEM of the cryoscopic fracture of copolymer with 10 wt % of Desmocap 12 cured at 70°C at both the center and the wall of the piece.

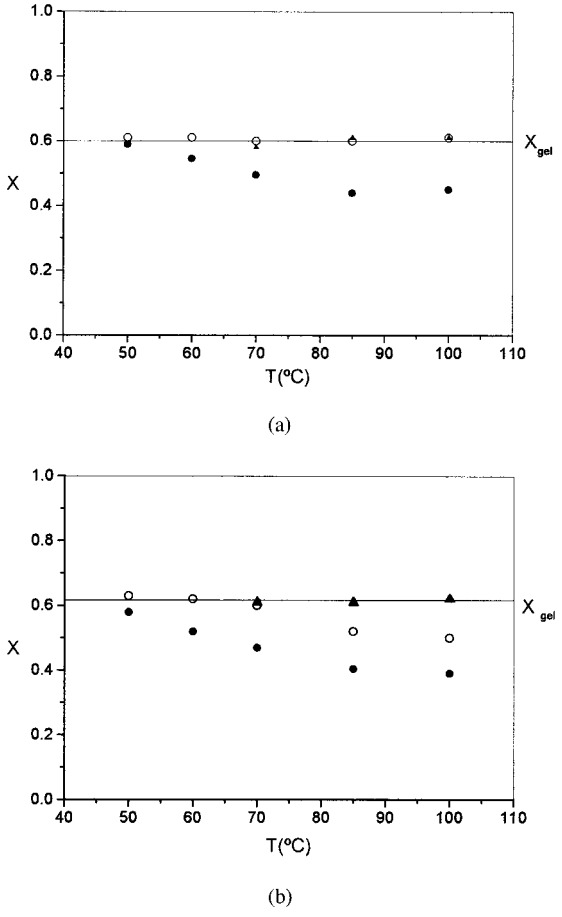

Figure 6 Cloud-point conversion versus temperature: (a) for the system with 10 wt % of Desmocap 12; (b) for the system with 20 wt % of Desmocap 12. (●) x_{CP}, (○) $x_{CP} + \Delta x_{CP}$, (▲) x_{GEL}.

Comparison of the spherical rubbery domains indicates that there is no important effect resulting from the different histories of temperature at the two positions analyzed. Comparison of the size of the inclusions in Figures 8(a) and 9(a) indicates that there is essentially no effect of the T_o in the temperature interval observed (70–100°C). Figures 9(a) and 9(b) confirm that the main variable that affects the size of the separated phase is the initial concentration of the urethane comonomer added to the system.[8,16,33]

Figure 10 shows the AFM image of the sample cured at 100°C with 20 wt % of modifier. Because of the higher resolution of the images obtained by AFM, it is possible to determine the roughness of the surface examined. Average roughness (AV) and peak-to-valley (PV) for the copolymers with 10 and 20 wt % of Desmocap 12 at two different oven temperatures (70 and 100°C) are shown in Table VI. AV and PV increase with the initial amount of prepolymer, a result that is in agreement with similar observations in a modified ep-

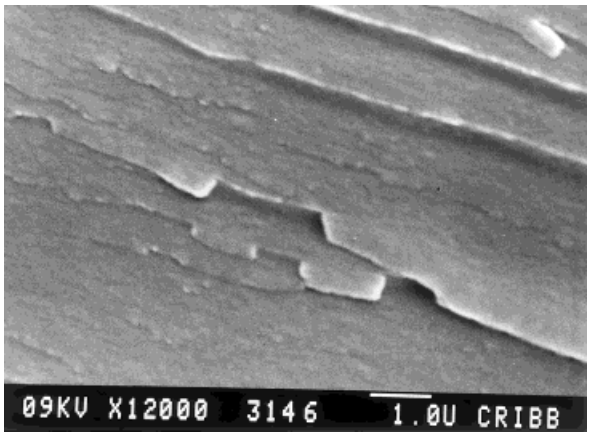

Figure 7 Morphology of the plaques modified with 10 wt % of Desmocap 12 and cured at oven temperature of 30°C (SEM).

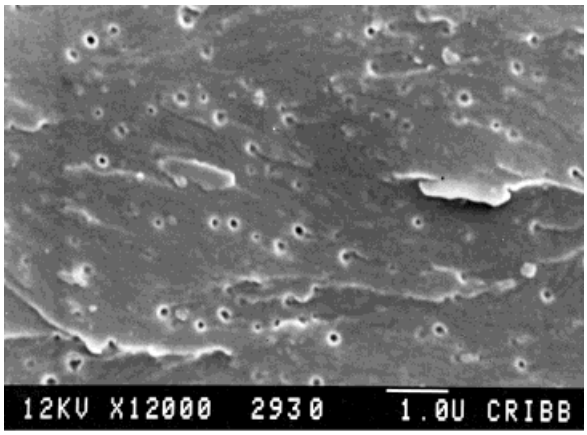

(a)

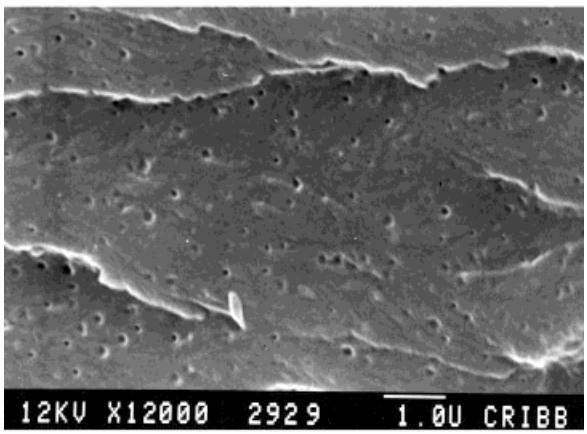

(b)

Figure 8 Morphology of the plaques modified with 10 wt % of Desmocap 12 and cured at oven temperature of 70°C (SEM): (a) center, (b) wall.

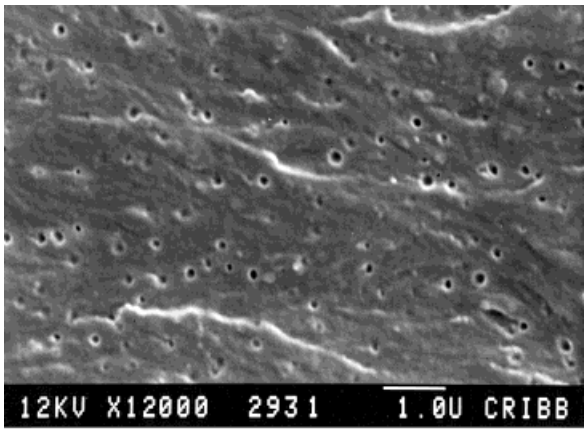

(a)

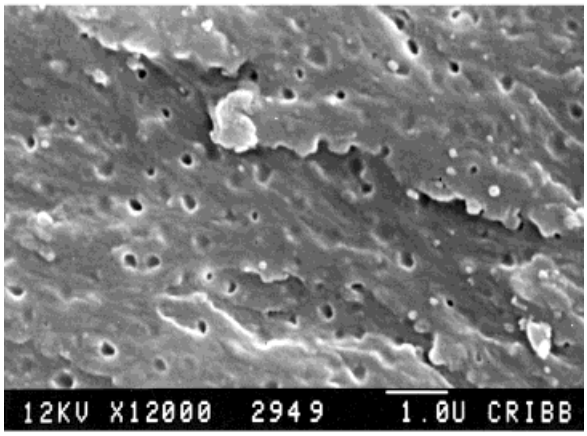

(b)

Figure 9 Morphology of the plaques modified with 10 wt % of Desmocap 12 and cured at oven temperature of 100°C, in the wall of plaque by SEM: (a) 10 wt % Desmocap 12; (b) 20 wt % Desmocap 12.

oxy system, as reported by Shaffer et al.[34] The authors analyzed the morphologies generated using SEM and AFM. They observed that as the size of the separated phase increases, the average and peak-to-valley roughness, measured by AFM, also increases.

Phase Diagrams

The formation of a heterogeneous structure and the glass transition of final copolymers can be explained using a conversion–temperature phase diagram. In that plot the vitrification and gelation curves are shown. $T_{g\infty}$ is the T_g of the system at complete conversion and ${}_{\text{gel}}T_g$ is the T at which the gelation curve intercepts the vitrification curve. Figure 11 shows such a plot for the epoxy–amine system with the conversion–temperature trajectories of the curing process (center and wall) indicated at two different conditions, with oven temperatures of 50 and 100°C. The vitrification conversion (x_V) and gel conversion (x_{gel}) versus temperature curves are also plotted. In the sample cured at 50°C, there is no important difference between center and wall conversion–temperature trajectories. The low T_g measured in this case (60°C for the center and wall) was the consequence, because vitrification took place at a conversion of about 0.7. The conversion–temperature trajectories of the sample cured at 100°C (center and wall) intercept the vitrification curve at values of conversion near to 1. A T_g of 122°C measured in the center of the sample, close to $T_{g\infty}$ (130°C) confirms that the sample was close to reach complete conversion.

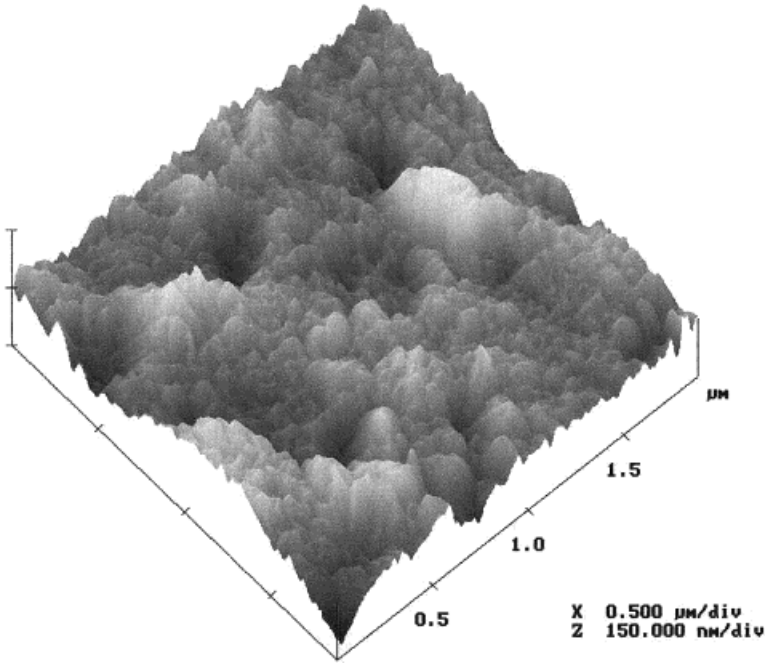

Figure 10 Morphology of the plaques modified with 20 wt % of Desmocap 12 and cured at oven temperature of 100°C, in the wall of plaques by AFM.

Figure 12 shows the phase diagram for the epoxy–amine system modified with 10 wt % of Desmocap 12, and cured at oven temperatures of 30, 70, and 100°C. The region where phase separation occurs is marked in the plots between the dashed line and x_{gel} at 10 wt % Desmocap 12 (Fig. 12) and between the two dashed lines at 20 wt % Desmocap 12 (Fig. 13). The two trajectories of the higher-temperature curves (T_{oven} = 70 and 100°C) cross the phase-separation region before reaching gelation. In these conditions the sample must phase separate, as was also observed in the morphology study of the samples. Although there is a difference in the temperature reached at the center and wall, microscopy did not show any noticeable difference of size and size distribution of the dispersed phase, probably because the conversions at which the separation took place are approximately the same at the two oven temperatures. The trajectory for the low-temperature cure (T_{oven} = 30°C) cross the vitrification curve before phase separation or gelation take place; thus, the sample should remain a one-phase material, as was also observed microscopically and by simple eye observation (transparent sample).

Figure 13 shows the phase diagram for the epoxy–amine system modified with 20 wt % of Desmocap 12. The features shown are similar to those of the previous system. Thus, if the sample is cured at 30°C, it remains homogeneous and it

Table VI Surface Statistics by AFM

T_o (°C)	Sample	Average Roughness[a] (nm)	Peak-to-Valley[b] (nm)
70	EA–10 wt % D12	45.433	421.16
	EA–20 wt % D12	56.241	698.61
100	EA–10 wt % D12	41.033	536.62
	EA–20 wt % D12	52.788	785.98

[a] Average roughness: mean values of the roughness curve line relative to the center line.
[b] Peak-to-valley: difference in height between the highest and lowest points over the length of the profile.

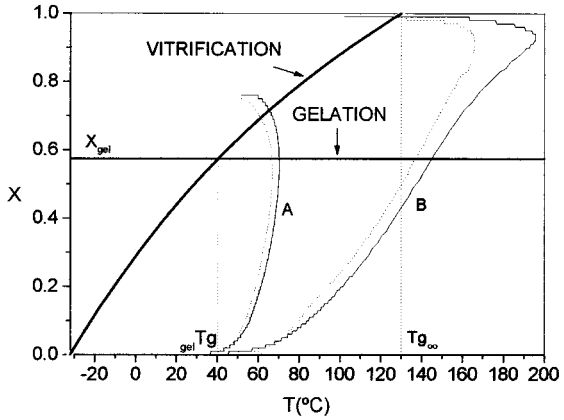

Figure 11 Phase diagrams for the epoxy–amine system. Conversion–temperature curves with oven temperatures of (A) 50°C, (B) 100°C. (· · ·) wall of plaque; (—) center of plaque.

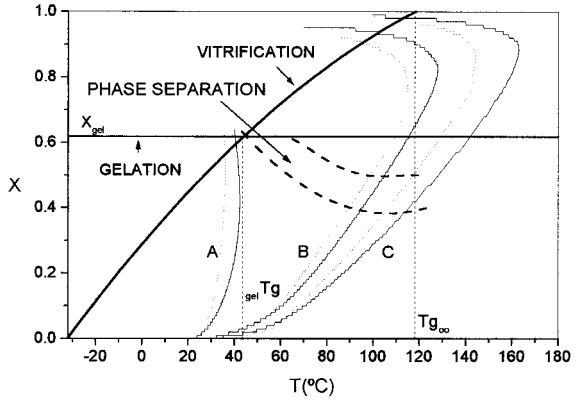

Figure 13 Phase diagrams for epoxy–amine–20 wt % Desmocap 12 system. Conversion–temperature curves with oven temperatures of (A) 30°C, (B) 70°C, (C) 100°C. (· · ·) wall of plaque; (—) center of plaque.

phase separates if it is cured at 70 or 100°C, although as mentioned before this process occurs at lower conversions.

CONCLUSIONS

The temperature–time trajectories at different positions of the sample thickness, oven temperature, percentage of modifier, and thickness of mold were measured.

The maximum temperature reached in the center of the mold and the difference in the wall temperature increases as the oven temperature increases and decreases with the amount of modifier used (dilution effect). Then, the difference between the T_g values in the center and the wall of the mold ($T_{g\ \text{center}} > T_{g\ \text{wall}}$) is in agreement with the temperature profile measured through the thickness of the sample.

SEM and AFM results correlate well and indicate that, in the present study, the initial concentration of PU elastomer is the main variable affecting the size of the rubbery domains phase-separated during curing.

The theoretical model, which includes the kinetic reaction and the effect of diffusion control at high conversions, allows reproduction of the temperature–time profiles in the plaques and prediction of the maximum conversion reached, even at low oven temperatures, where the vitrification effect is more important. The low final conversion reached at low oven temperatures is in agreement with the low T_g values measured in the plaques.

The superposition of the phase diagrams with the conversion–temperature trajectories followed by the sample during the curing explains the different morphologies generated. At low oven temperatures (30°C) the sample does not separate in phases and the material remains homogeneous (transparent). At higher oven temperatures (70 and 100°C) the conversion–temperature trajectories cross the phase separation region before reaching gelation. However, the size of the dispersed phase increased significantly only with the initial amount of modifier. There was no difference in the size of the dispersed phase with the position in the mold.

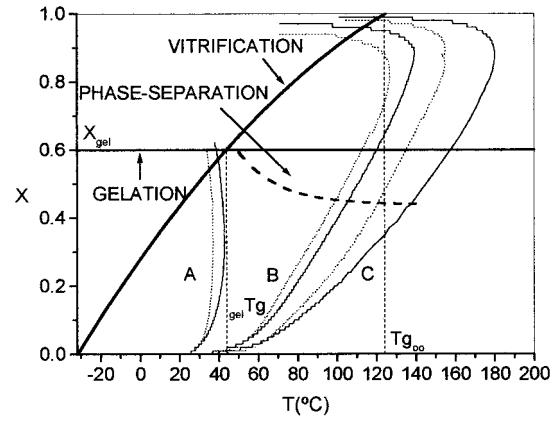

Figure 12 Phase diagrams for epoxy–amine–10 wt % Desmocap 12 system. Conversion–temperature curves with oven temperatures of (A) 30°C, (B) 70°C, (C) 100°C. (· · ·) wall of plaque; (—) center of plaque.

The authors thank CONICET (National Research Council of Argentina) for the financial support and especially for the fellowship awarded to P.M.S.

REFERENCES

1. Verchère, D.; Pascault, J. P.; Sautereau, H.; Moschiar, S. M.; Riccardi, C. C.; Williams, R. J. J. J Appl Polym Sci 1991, 43, 293.
2. Bussi, P.; Ishida, H. J Appl Polym Sci 1994, 53, 441.
3. Huang, Y.; Kinloch, A. J. Polymer 1992, 33, 1330.
4. Huang, Y.; Kinloch, A. J. J Mater Sci Lett 1992, 11, 484.
5. Huang, Y.; Hunston, D. L.; Kinloch, A. J.; Riew, C. K. in Toughened Plastic, Vol. 1; Riew, C. K.; Kinloch, A. J., Eds.; American Chemical Society: Washington, DC, 1993; Chapter 1.
6. Bandyopadhyay, S. in Toughened Plastic, Vol. 1; Riew, C. K.; Kinloch, A. J., Eds.; American Chemical Society: Washington, DC, 1993; Chapter 9.
7. Kinloch, A. J.; Shaw, S. J.; Tod, D. A.; Hunston, D. L. Polymer 1983, 24, 1355.
8. Kinloch, A. J.; Hunston, D. L.; J Mater Sci Lett 1987, 6, 131.
9. Bucknall, O. B.; Yoshit, T. Br Polym J 1978, 10, 53.
10. Lanzetta, N.; Laurienzo, P.; Malinconico, M.; Martuscelli, E.; Rasgosta, G.; Volpe, M. G. J Mater Sci 1992, 27, 786.
11. Yee, A. F.; Pearson, R. A. J Mater Sci 1986, 21, 2462.
12. Pearson, R. A.; Yee, A. F. J Mater Sci 1986, 21, 2475.
13. Visconti, S.; Marchessault, R. H. Macromolecules 1974, 7, 913.
14. Ruseckaite, R. A.; Hu, L.; Riccardi, C. C.; Williams, R. J. J. Polym Int 1983, 30, 287.
15. Grillet, A. C.; Galy, J.; Pascault, J. P. Polymer 1992, 33, 34.
16. Moschiar, S. M.; Riccardi, C. C.; Williams, R. J. J.; Verchère, D.; Sautereau, H.; Pascault, J. P. J Appl Polym Sci 1991, 42, 717.
17. Bussi, P.; Ishida, H. J Polym Sci Part B Polym Phys 1994, 32, 647.
18. Huang, Y.; Kinloch, A. J.; Bertsh, R. J.; Siebert, A. R. in Toughened Plastic, Vol. 1; Riew, C. K.; Kinloch, A. J., Eds.; American Chemical Society: Washington, DC, 1993; Chapter 8.
19. Fang, D. P.; Frontini, P. M.; Riccardi, C. C.; Williams, R. J. J. Polym Eng Sci 1995, 35, 1358.
20. Reboredo, M. M.; Vazquez, A. Polym Eng Sci 1995, 35, 1521.
21. Williams, R. J. J. in Developments in Plastic Technology, Vol. 2; Welar, A.; Craft, J., Eds.; Elsevier Applied Science: London, 1985; p. 339.
22. Mijovich, J.; Wang, H. T. SAMPE J 1988, March/April, 42.
23. Chater, M.; Bouzon, J.; Vergnaud, J. M. Plast Rubber Compos Process Appl 1987, 7, 199.
24. Stefani, P. M.; Moschiar, S. M.; Aranguren, M. I. J Appl Polym Sci 2001, 79, 1771.
25. Rabinowitch, F. Trans Faraday Soc 1937, 33, 1225.
26. Adam, G.; Gibbs, J. H. J Chem Phys 1965, 43, 139.
27. Nielsen, L. E. J Macromol Sci Rev Macromol Chem 1969, C3, 69.
28. Pascault, J. P.; Williams, R. J. J. J Polym Sci Part B Polym Phys 1990, 28, 85.
29. Pascault, J. P.; Williams, R. J. J. Polym Bull 1990, 24, 115.
30. Maistros, G. M.; Bucknall, C. B. Polym Eng Sci 1994, 34, 1517.
31. Williams, R. J. J.; Benavente, M. A.; Ruseckaite, R. A.; Churio, M. S.; Hack, H. G. Polym Eng Sci 1990, 30, 1140.
32. Girard–Reydet, F.; Riccardi, C. C.; Sautereau, H.; Pascault, J. P. Macromolecules 1995, 28, 7599.
33. Montarnal, S.; Pascault, J. P.; Sautereau, H. in Rubber-Toughened Plastics; Riew, C. K., Ed.; American Chemical Society: Washington, DC, 1989; p. 193.
34. Shaffer, O. L.; Bagheri, R.; Qian, J. Y.; Dimonie, V.; Pearson, R. A.; El-Aasser, M. S. J Appl Polym Sci 1995, 58, 465.